

Supporting Information

Bioinspired redox-coupled conversion reaction in FeOOH-acetate hybrid nanoplatelets for Na ion battery

Bum Chul Park[†], Jiung Cho[†], Jiliang Zhang[†], Mawuse Amedzo-Adore, Dae Beom Lee, Sung-Chul Kim, Jong Seong Bae, Young Rang Uhm, Sang-Ok Kim, Jehyoung Koo, Yong-Mook Kang^{}, and Young Keun Kim^{*}*

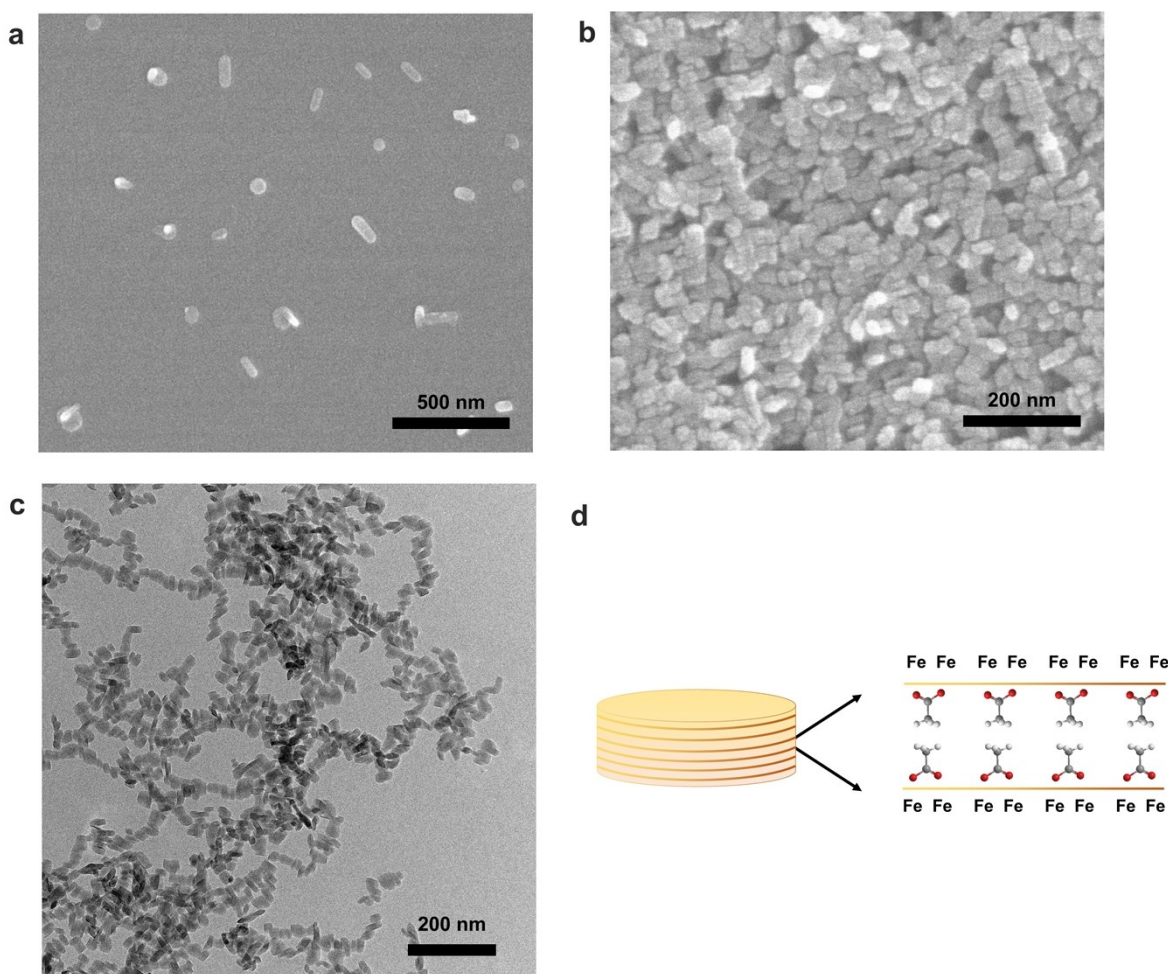


Figure S1. Morphological analysis of FAHP. (a) Low- and (b) high-magnification SEM images of FAHP. (c) Low-magnification TEM image of FAHP. FAHP tends to agglomerate in the [010] direction coincident with the stacking direction of the sheet. **d**, Schematic illustration of FAHP in which organic and inorganic components are stacked in a layer-by-layer assembly.

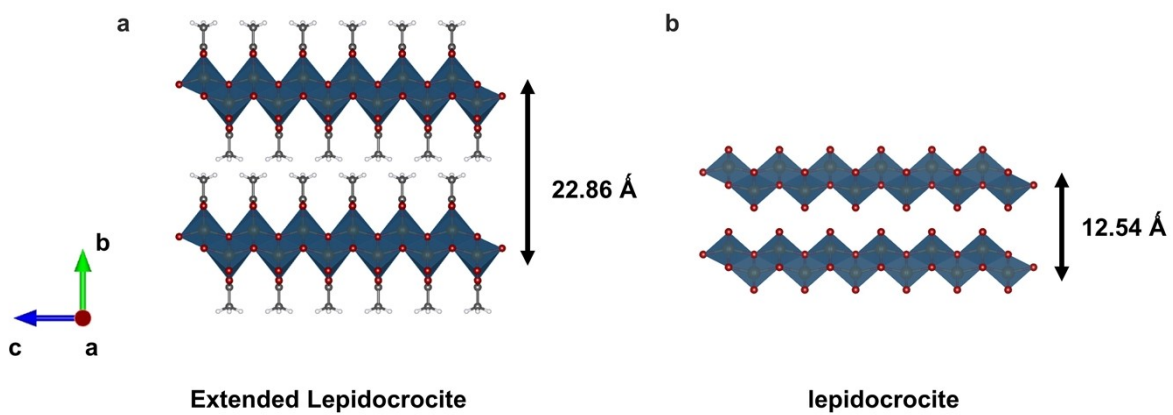


Figure S2. Crystal structures. (a) FAHP. (b) Lepidocrocite.

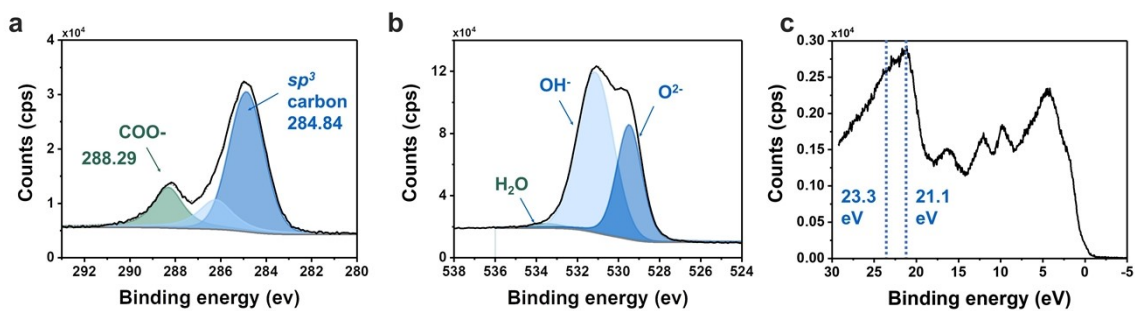


Figure S3. Surface analyses of FAHP. (a) Deconvoluted O 1s XP spectra with peaks marked as COO⁻ (green), CO-Fe (sky blue), and *sp*³ C (blue) in the order of increasing BE. (b) Deconvoluted O 1s XP spectra with peaks marked as H₂O (green), OH⁻ (sky blue), and O²⁻ (blue) in the order of increasing BE. (c) O 2p and valence XP spectra. The peaks in the range of O 2p were marked at 23.3 and 21.1 eV.

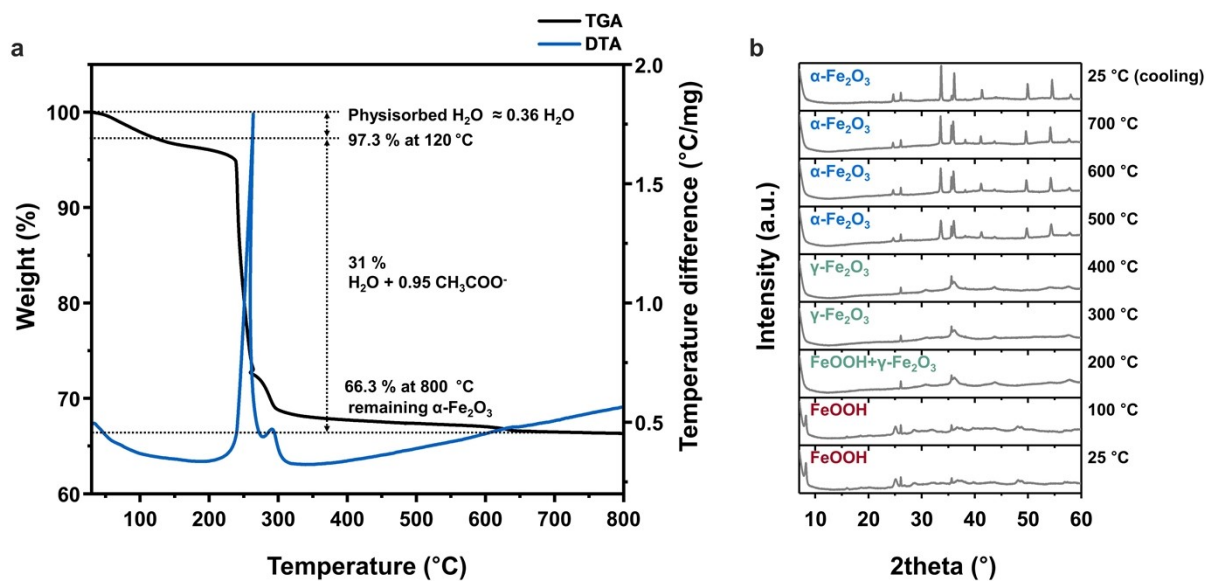


Figure S4. Composition analyses using thermal phase transformation of FAHP. (a) Results of thermogravimetric and differential thermal analysis of FAHP conducted in a flow of air. Dotted lines indicate the decomposed elements in the corresponding temperature ranges. (b) In situ thermal XRD patterns of FAHP recorded in a flow of air. The XRD patterns were recorded at temperature intervals of 100 °C while heating up to 700 °C and after cooling to room temperature. The phases of iron oxide produced at each temperature were noted: FeOOH·0.5CH₃COO (25 and 100 °C) → γ-Fe₂O₃ (200, 300, and 400 °C) → α-Fe₂O₃ (500, 600, and 700 °C).

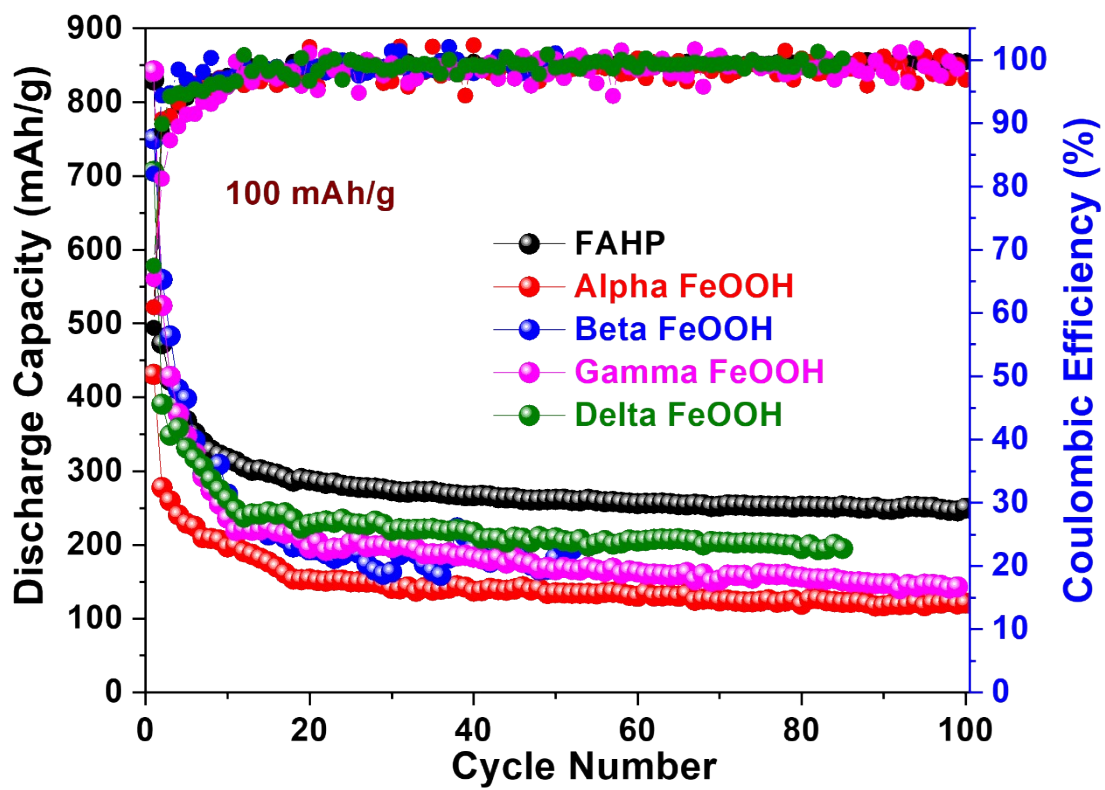


Figure S5. Cycle retention of FAHP and FeOOH at 100 mA g^{-1} .

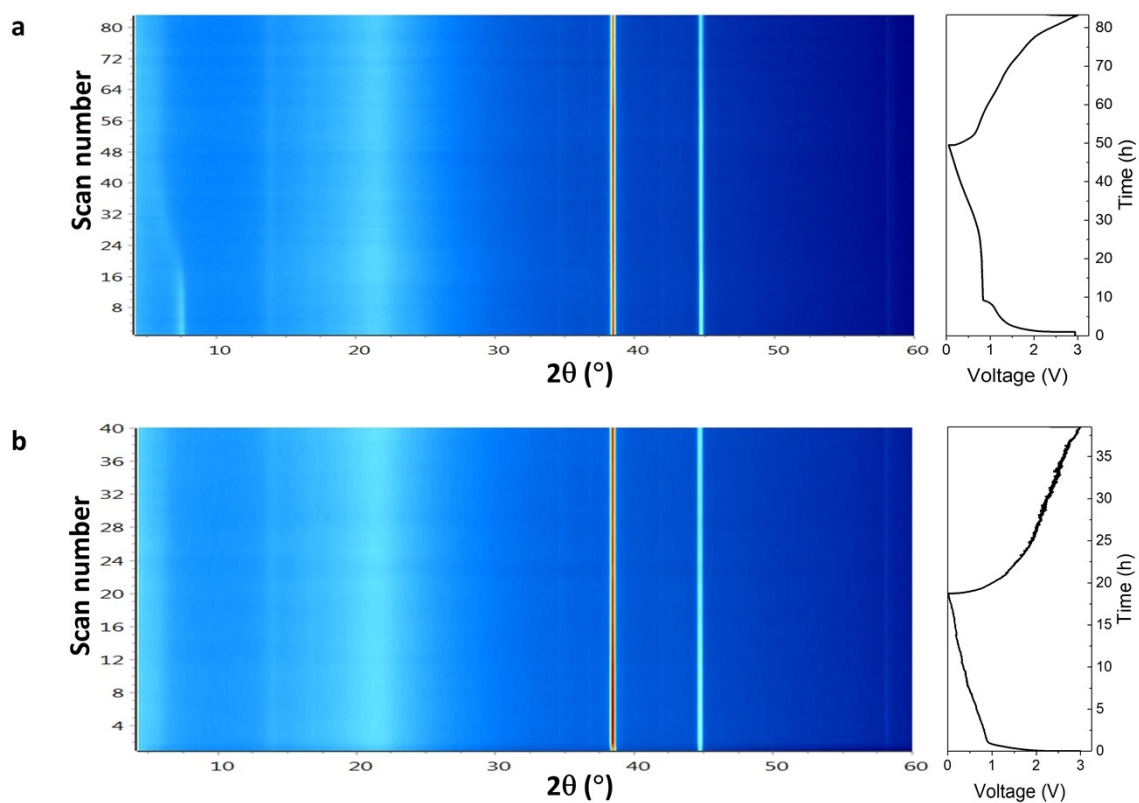


Figure S6. 2D in situ XRD analyses. In situ XRD patterns of the FAHP electrode (a) during the initial cycles within the potential range of 0.01–3.0 V at a current density of 20 mA g⁻¹ and (b) at the end of the 10th cycle. During the cycling process, a single XRD pattern was recorded over 1 h. The color bars indicate the peak intensity of the XRD pattern.

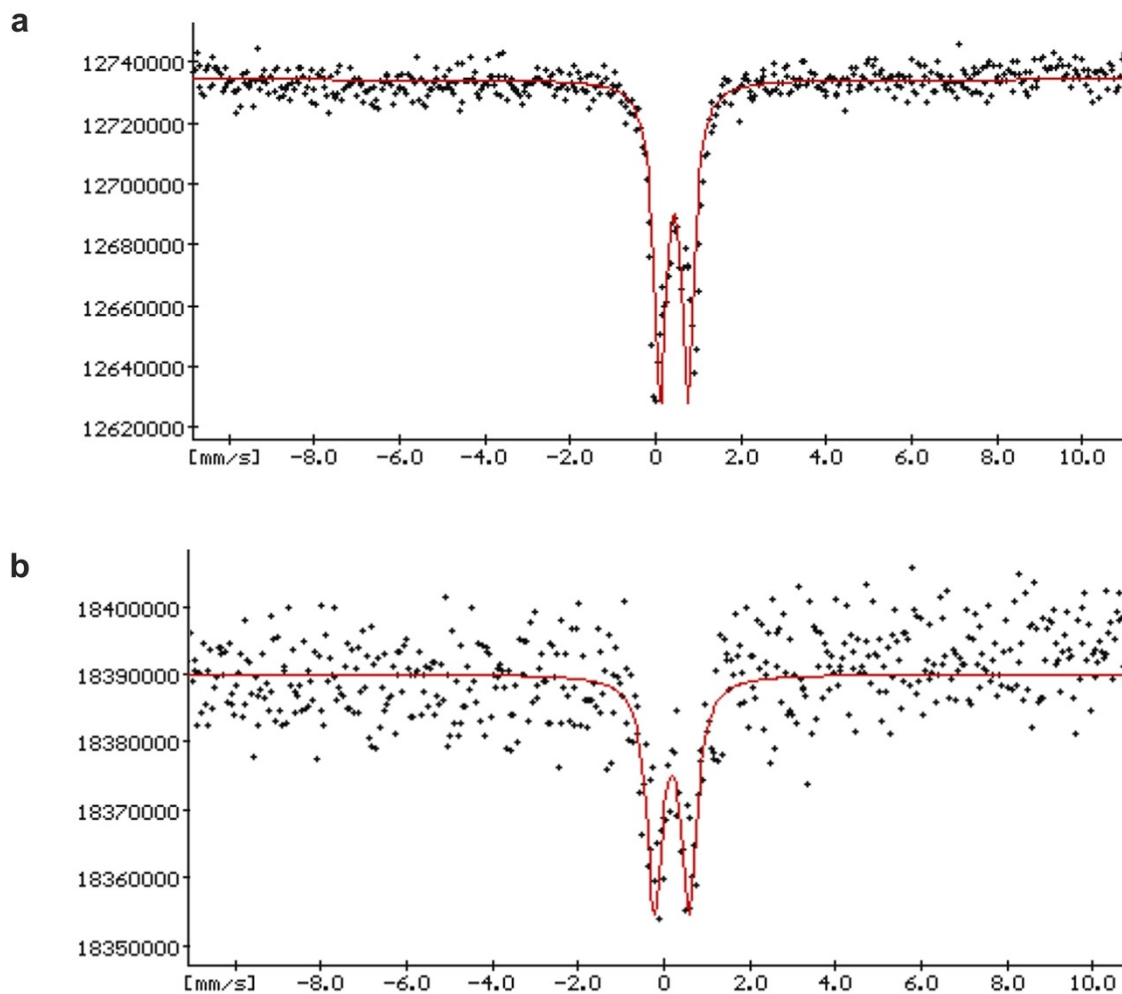


Figure S7. Mössbauer spectra of (a) FAHP powder with an isomer shift of 0.41 mm s^{-1} (electrode) and quadrupole splitting of 0.65 mm s^{-1} ($\gamma\text{-FeOOH}$), (b) first sodiated FAHP electrode with an isomer shift of 0.3 mm s^{-1} (electrode) and quadrupole splitting of 0.8 mm s^{-1} (Fe_3O_4). The Mössbauer spectra of the samples were fitted to a doublet.

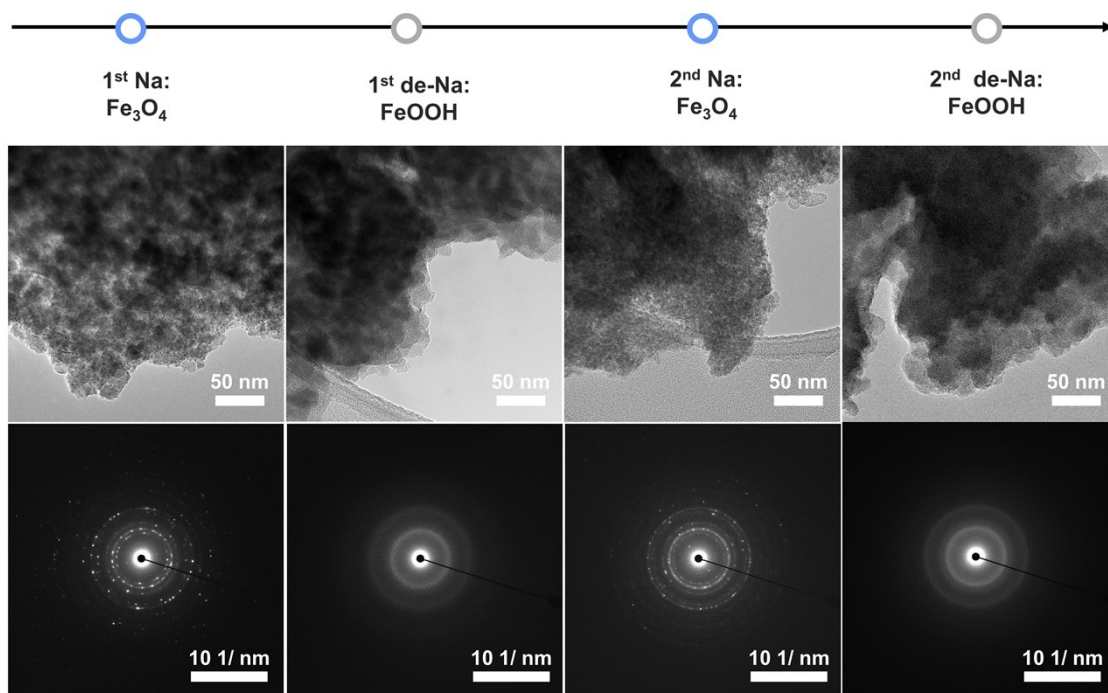


Figure S8. Phase transformation of FAHP upon the conversion reaction. Ex situ bright-field TEM images and SAED patterns of the cycled electrode following the first and second discharge–charge cycles. The clear ring patterns at $d = 2.83, 2.53, 2.51, 1.42, 1.20,$ and 1.01 nm obtained from the sodiated samples indicate the presence of crystalline Fe_3O_4 phases. The diffuse ring patterns at $d = 2.15$ and 1.52 nm obtained from the desodiated samples indicate the presence of poorly crystalline FeOOH phases.

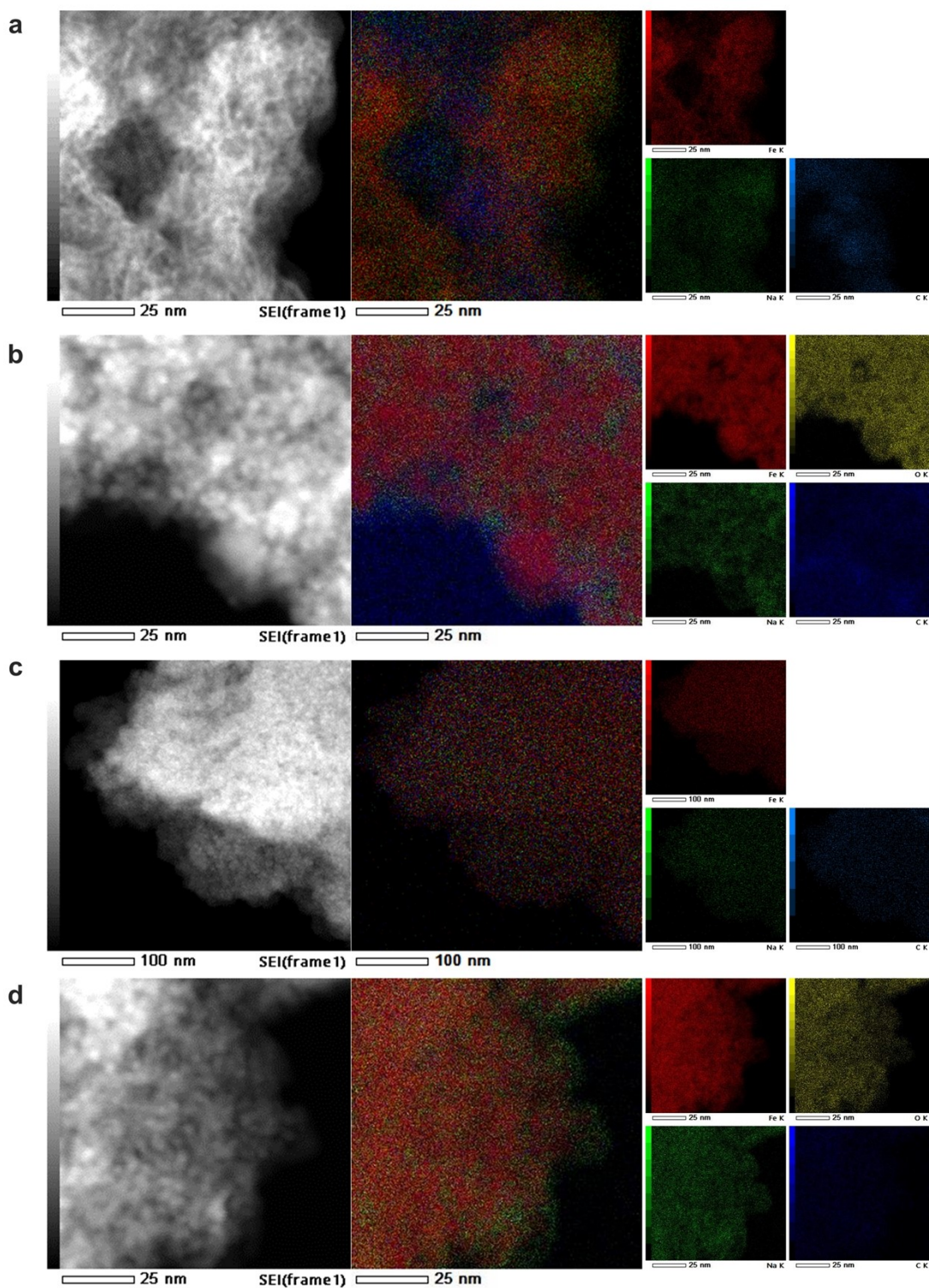


Figure S9. Elemental analysis of the conversion reaction. Ex situ EDS elemental maps of the cycled electrode at different reaction stages: (a) 0.5 V in discharge, (b) initial complete discharge, (c) initial complete charge, and (d) second fully discharge. Each atomic element is marked with a different color: Fe (red), Na (green), O (yellow), and C (blue).

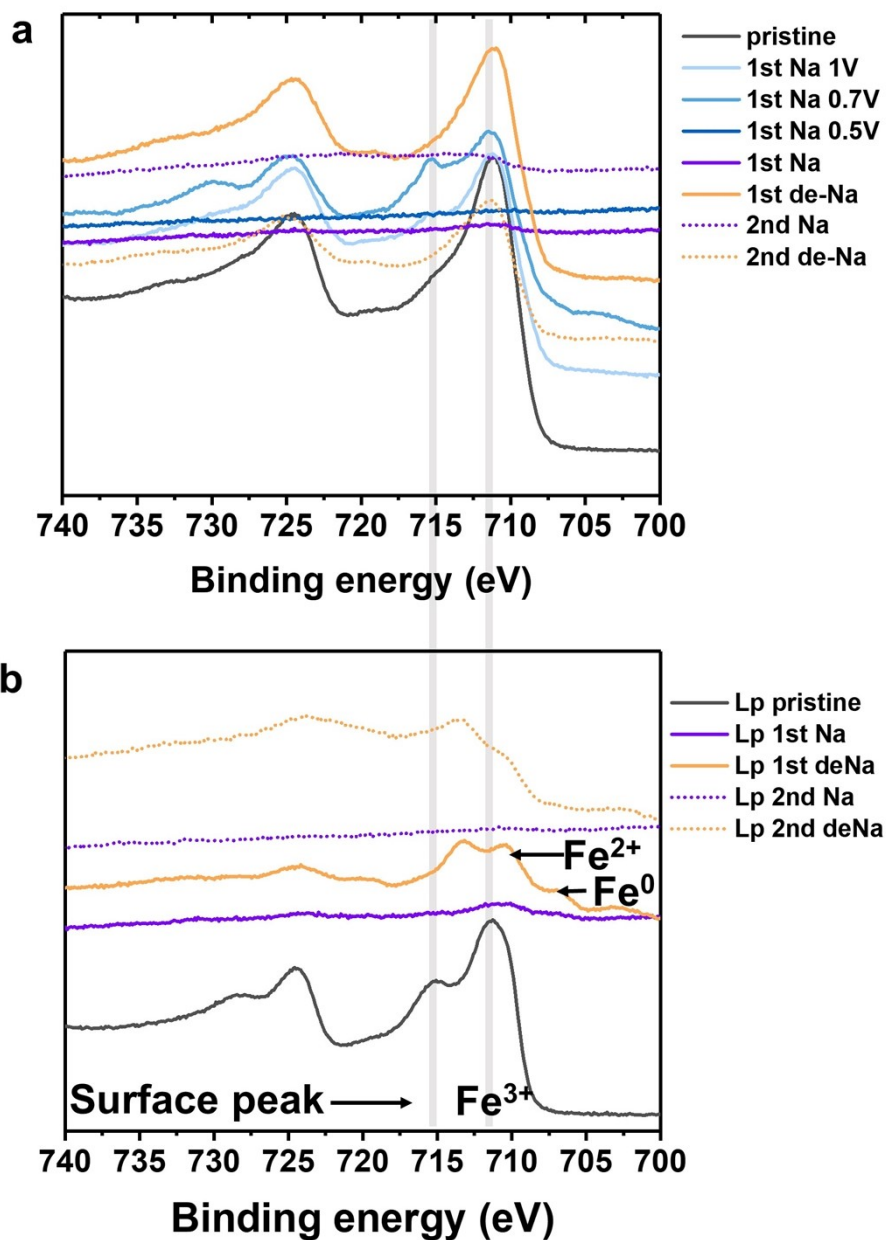


Figure S10. Conversion reaction from Fe_{2p} XP spectra. Fe_{2p} XPS profiles of (a) FAHP and (b) lepidocrocite.

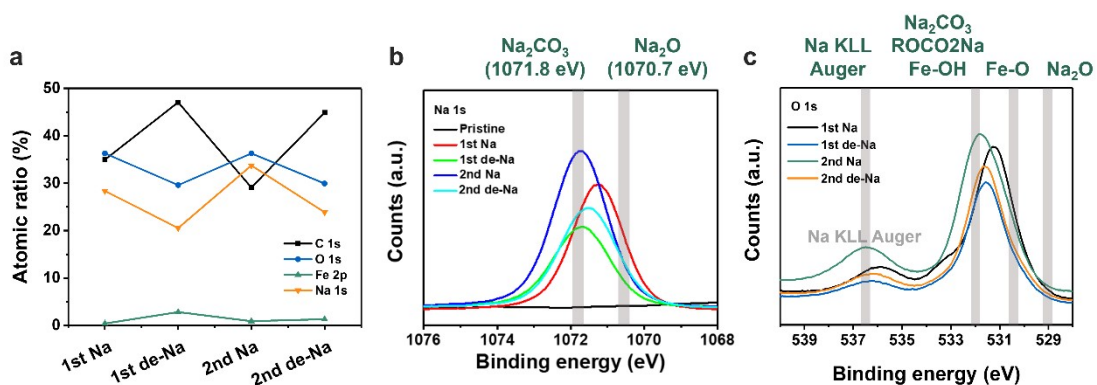


Figure S11. Surface analysis results. (a) Compositional XPS survey of discharge-charge cycling. (b) Na 1s XPS profile recorded during discharge-charge cycling. The peak at 1071.8 eV assigned to Na_2CO_3 was more intense than the peak originated from Na_2O (1070.7 eV). (c) O 1s XPS profile recorded during discharge-charge cycling. Na_2O did not contribute significantly to the O 1s profile.

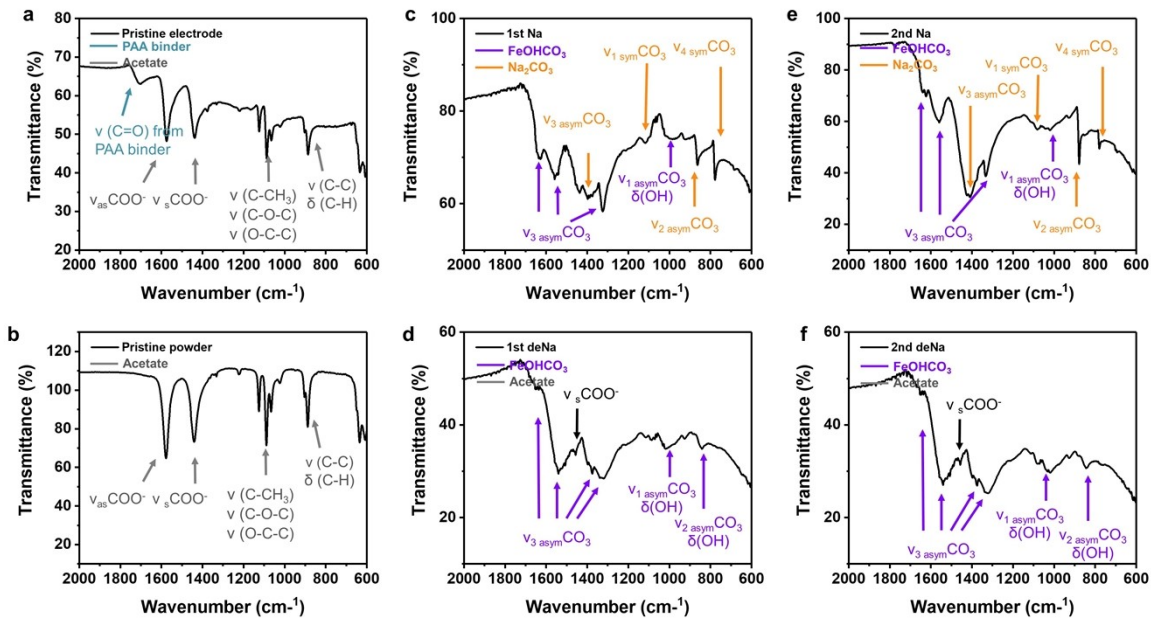


Figure S12. FT-IR spectroscopy results. FT-IR spectra of (a) pristine FAHP, (b) pristine electrode, (c) initially sodiated electrode, (d) initially desodiated electrode, (e) second sodiated electrode, and (f) second desodiated electrode in the wavenumber range lower than 2000 cm^{-1} . The vibration modes for each spectrum are colored as gray (acetate), green (PAA binder), purple (HCO_3^- coordinated on FeOOH surface), and orange (Na_2CO_3) solid arrows.

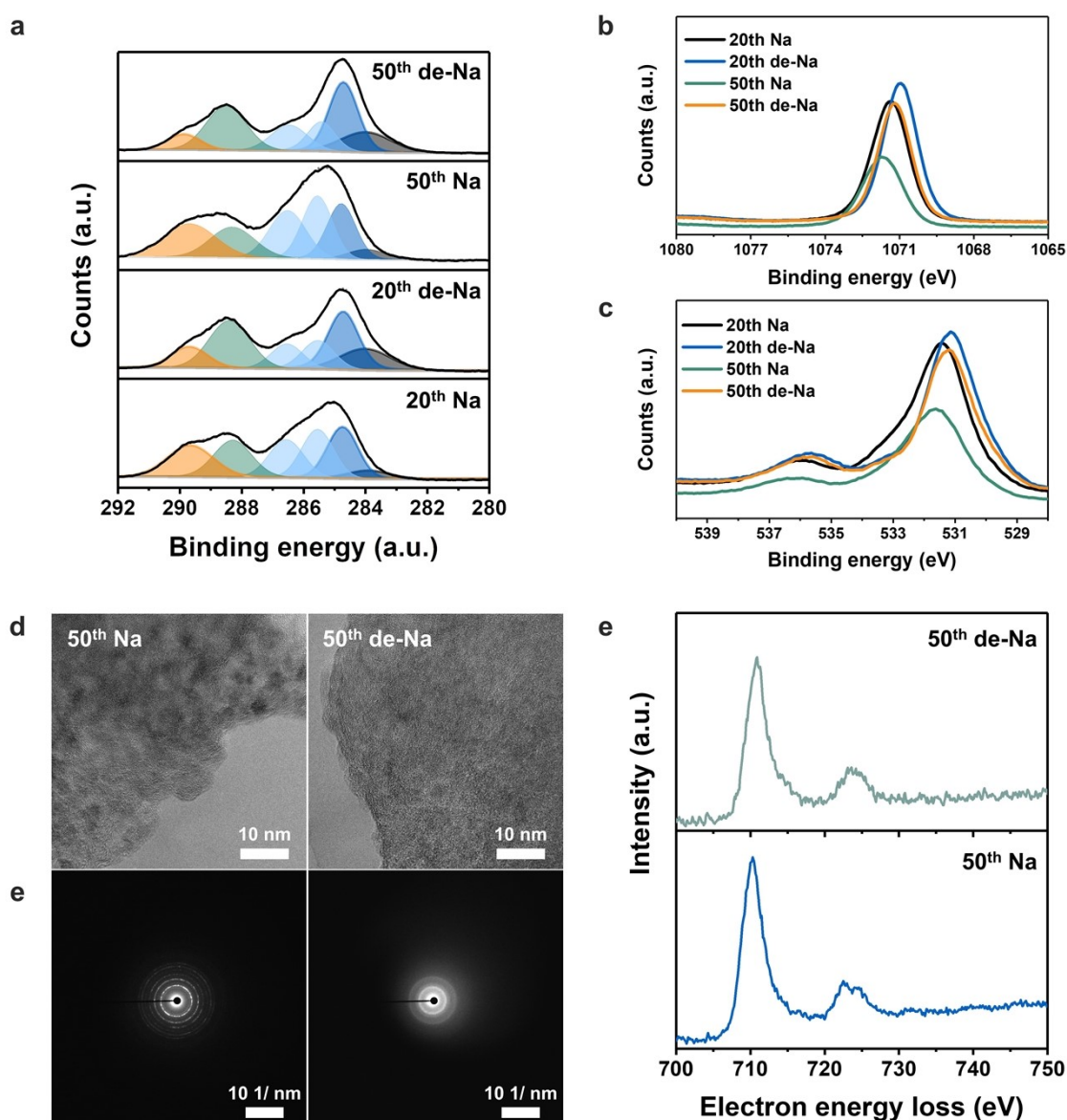


Figure S13. Conversion reaction analyses over the 20th and 50th cycles. (a) C1s XPS spectra recorded at the completely discharged and charged stages of the 20th and 50th cycles. Deconvoluted peaks marked as Na₂CO₃ (orange), COO⁻ (green), CO-Fe (sky blue), and sp³ C (blue), and sp² C (gray) in the order of increasing BE. Na₂CO₃ remained in all samples; however, its proportion dominated in the discharged samples, maintaining the reversibility of Na₂CO₃ formation and dissolution. (b) Na 1s and (c) O1s XPS spectra at completely discharged and charged stages of the 20th and 50th cycles, which coincide with the first and second cycles. (d) HR-TEM images, (e) SAED patterns, and (f) and EEL spectra (f) at the 50th cycle. Even in the 50th discharge–charge process, the conversion reaction from crystalline Fe₃O₄ to poorly crystalline FeOOH occurred. In particular, following the 20th and 50th cycles, Na₂CO₃ was partially stabilized; however, the formation and dissolution of Na₂CO₃ were repeated. Furthermore, continuous cycling slightly refined the size of the Fe₃O₄ crystallite (<5 nm).

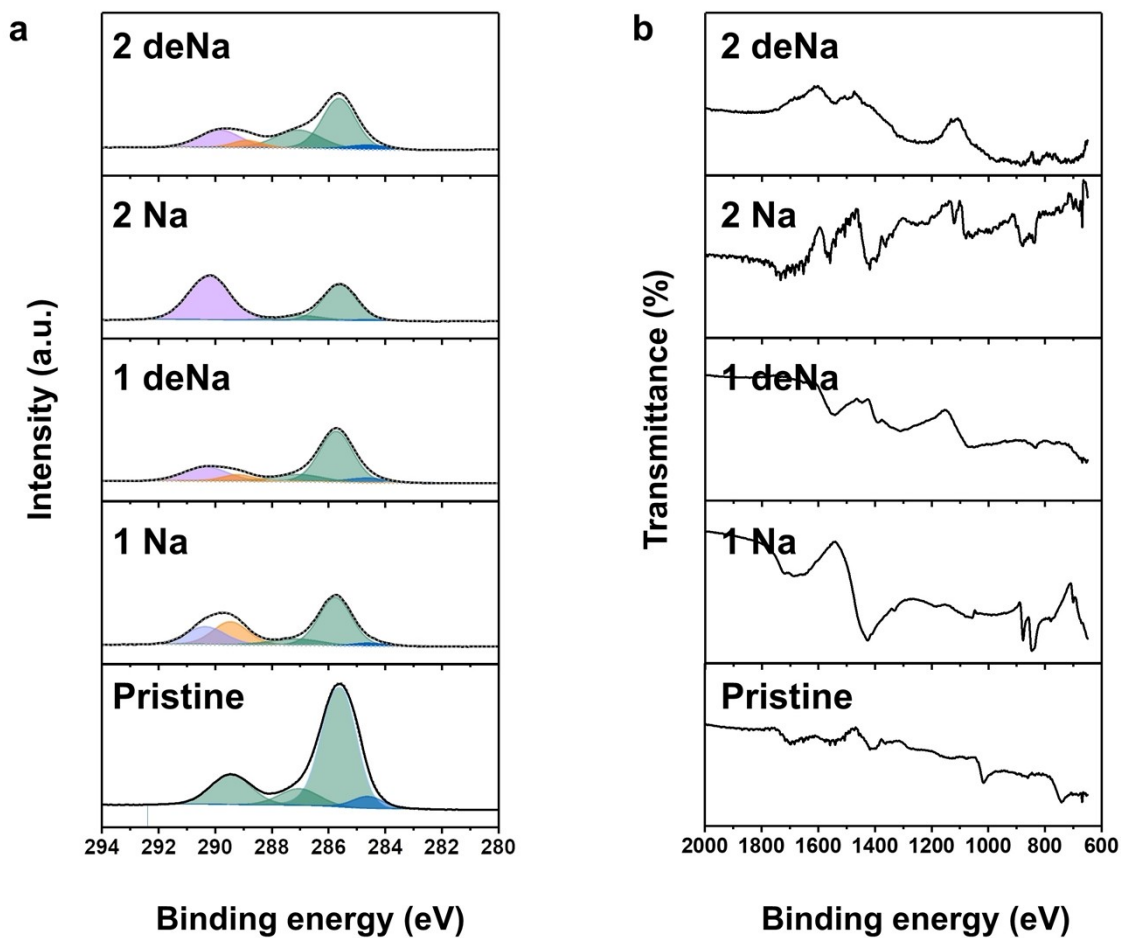


Figure S14. Surface reaction of lepidocrocite. (a) C1s XPS profiles and (b) FT-IR spectra of lepidocrocite during discharge–charge processes. Deconvoluted peaks in the C1s XP spectra marked as bicarbonate (purple), carbonate (orange), oxidized carbon (green), and sp^3 C (blue).

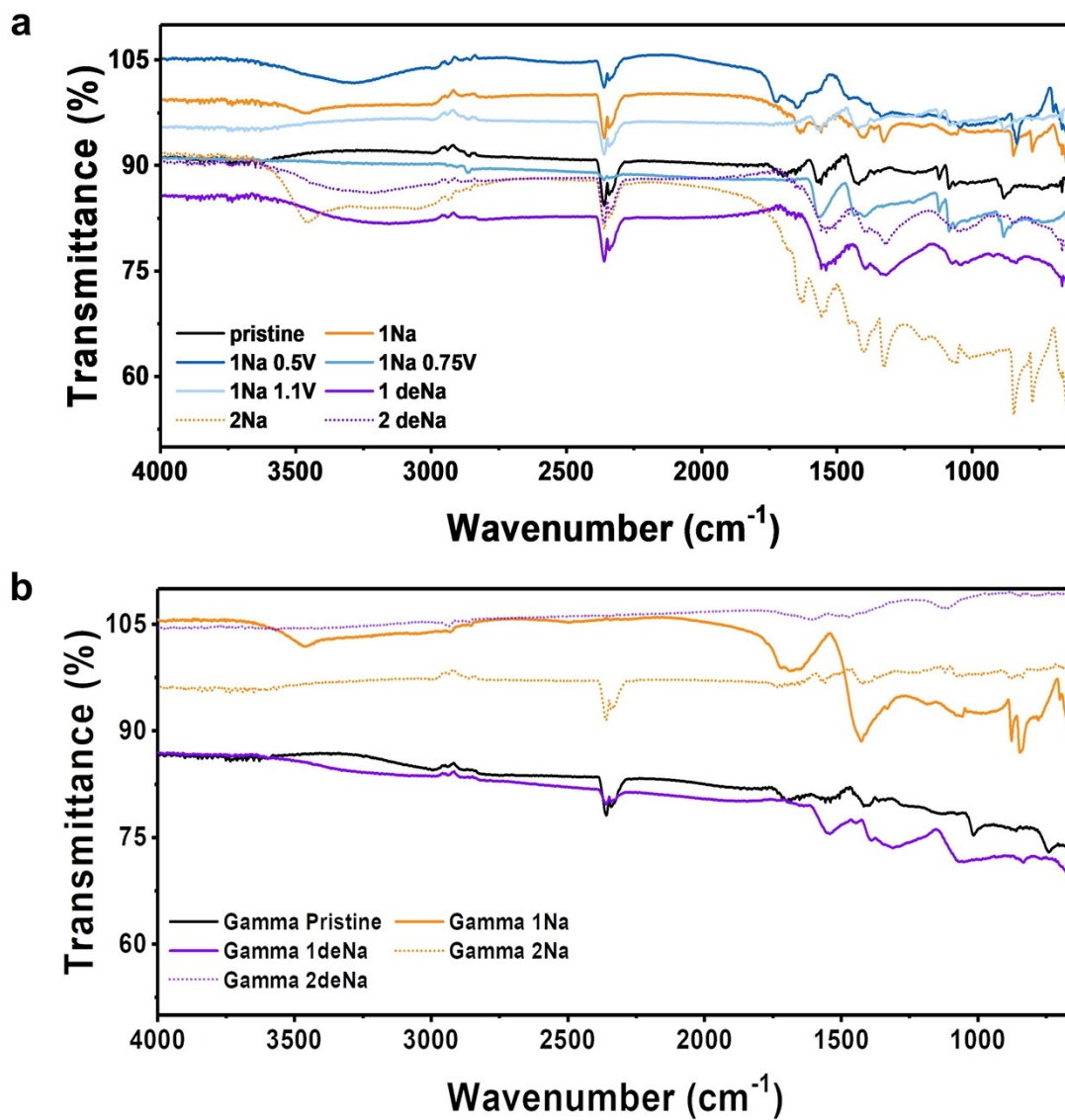


Figure S15. Surface reaction between FAHP and lepidocrocite. FT-IR spectra of (a) FAHP and (b) lepidocrocite recorded during the discharge–charge processes.